Recurrence spectra of a helium atom in parallel electric and magnetic fields

Dehua Wang[1,2] and Shiliang Ding[1,*]
[1]*School of Physics and Microelectronics, Shandong University, Jinan 250100, People's Republic of China*
[2]*Department of Mathematics and Physics, Shandong Architecture and Engineering Institute, Jinan 250014, People's Republic of China*

(Received 10 March 2003; published 22 August 2003)

A model potential for the general Rydberg atom is put forward, which includes not only the Coulomb interaction potential and the core-attractive potential, but also the exchange potential between the excited electron and other electrons. Using the region-splitting consistent and iterative method, we calculated the scaled recurrence spectra of the helium atom in parallel electric and magnetic fields and the closed orbits in the corresponding classical system have also been obtained. In order to remove the Coulomb singularity of the classical motion of Hamiltonian, we implement the Kustaanheimo-Stiefel transformation, which transforms the system from a three-dimensional to a four-dimensional one. The Fourier-transformed spectra of the helium atom has allowed direct comparison between peaks in such a plot and the scaled action values of closed orbits. Considering the exchange potential, the number of the closed orbits increased, which led to more peaks in the recurrence spectra. The results are compared with those of the hydrogen case, which shows that the core-scattered effects and the electron exchange potential play an important role in the multielectron Rydberg atom.

DOI: 10.1103/PhysRevA.68.023405 PACS number(s): 32.60.+i

I. INTRODUCTION

Highly excited atoms in strong external fields have been shown to be the real physical examples of the nonintegrable systems to study the quantum manifestations of classical chaos both experimentally and theoretically. Gutzwiller's semiclassical trace formula for the quantum density of states and closed-orbit theory [1] introduced new ways of looking at the photoabsorption spectrum of Hamiltonians having chaotic classical dynamics. For light atoms, such as hydrogen and the negative hydrogenic ion, in strong external fields, the closed-orbit theory has proven to be a quantitative and elegant method of calculating and interpreting the recurrence spectra [2]. However, a complete theoretical treatment of multielectron atoms in external fields remains a challenge. Recent works have found that the effects of a nonhydrogenic ionic core should be taken into account [3]. Following quantum-defect theory, the electron-core interactions are characterized by a set of energy independent quantum defects. Such results predict when the ionic effects of the multielectron atom are included, the new recurrence peaks called core-scattered recurrences [4] emerge in large numbers. These appear as a result of one primitive closed orbit of period T_1 scattering into another of period T_2 to produce a new peak at the combined period T_1+T_2, thus causing the combination orbits. For lithium, both theory and experiment have confirmed the existence of these nonclassical core-scattered features [3].

Starting with the physical picture of the photoabsorption process suggested by Gao and Delos [5] and including the core-scattered waves consistently, we have recently been able to extend the closed-orbit theory to successfully reproduce the core-induced phenomena [3]. The advantage of our semiclassical approach is that it allows us to describe the dynamics of the relatively complicated multielectron systems in terms of the system which is simple, yet closely related to the hydrogenic system.

To date, many researchers have studied the recurrence spectra of He atom. But they only calculated the spectra of the He atom in singular electric or magnetic field [8–12], as for the coexistence of electric and magnetic fields, no one has yet studied. In this paper, we present theoretical computations of the recurrence spectra of the helium atom in strong, parallel, external electric and magnetic fields by using a model potential, which includes not only the Coulomb interaction potential and the core-attractive potential, but also the exchange potential between the excited electron and other electrons. We have used the closed-orbit theory and the region-splitting consistent and iterative method developed by Dondo *et al.* [4]. Matching the quantum Coulomb wave near the nucleus to the semiclassical wave constructed by using a new scale property and the Kustaanheimo-Stiefel transformation [7], the Coulomb singularity of the classical motion has been removed and the corresponding spectra between the theoretical and experimental results are obtained, we reveal a new insight in the classical interpretation of quantum photoabsorption spectra.

This paper is organized as follows: In the following section, we put forward a model potential for the general Rydberg atom, in particular, the potential of the He Rydberg atom. In Sec. II, we analyze how the closed-orbit theory can be extended to include the core-scattered contributions consistently and the region-splitting consistent and iterative method. Section IV gives the equation for calculating the recurrence spectra of the He atom in parallel electric and magnetic fields at constant scaled energy. In Sec. V, we calculate the recurrence spectra and compare it with those of the hydrogen case by using the closed-orbit theory. Section VI gives some conclusions of this paper.

*Author to whom correspondence should be addressed. Email address: shlaudin@sdu.edu.cn

II. MODEL POTENTIAL FOR THE GENERAL RYDBERG ATOM

For the general Rydberg atom, where only one electron is highly excited to the ionization threshold while the ionic core remains in the ground state. In this situation, the nuclear charge is screened by the inner electrons. Thus, in the previous study, some researchers consider that the potential acting on the excited electron is an attractive Coulomb potential modified by a short-ranged core potential [4], but neglect the influence of the exchange interaction potential. The exchange interaction is isolated experimentally by measuring recurrence spectra versus spin state. This provides a tool to examine the role of the Pauli exclusion principle in the semiclassical theory and in the dynamics of Rydberg systems, where it is not well understood. Closed orbits are sensitive to the spin-dependent exchange interaction since the Rydberg electron approaches the core, it moves as if it experiences an attraction or repulsion depending on the relative orientation of the two spins. This introduces a coupling between the spatial variables of the Rydberg electron and the spin state of the atom. Keeler and Morgan [12] have studied the influence of the electron exchange on the recurrence spectra of He atom experimentally, but they did not give an effective potential to model the influence of the exchange interaction. Considering the influence of the exchange interaction, we present a model potential in this paper.

For the Rydberg atom, the potential acting on the excited electron is the total interaction energy of this electron with the nucleus and other electrons. It may be formulated as

$$V(r)=V_n+V_{\mathrm{core}}+V_{\mathrm{ex}}. \tag{1}$$

V_n is the nucleus-attractive potential to the excited electron:

$$V_n=-\frac{z}{r}, \tag{2}$$

where z is the charge of the nucleus. V_{core} is a short-ranged Coulomb interaction potential between the excited electron and the other electrons:

$$V_{\mathrm{core}}=e^2\int\int\frac{\rho(r_i)\rho(r_j)}{r_{ij}}d\tau_i d\tau_j, \tag{3}$$

where $\rho(r_i)=\Sigma_i|\psi_i|^2$ is the density function of the ith electron [13], $\psi_i(r)$ is the wave function of the electron; r_{ij} is the distance between the ith and the jth electron. For the He Rydberg atom, one electron lies in the ground state while another electron was excited to the $2s$ state, then

$$V_{\mathrm{core}}=\frac{2}{r}-\left(\frac{1}{r}+2\right)e^{-4r}-\left(\frac{1}{r}+\frac{3}{2}+r+r^2\right)e^{-2r}. \tag{4}$$

V_{ex} is the exchange potential between this α-spin electron and the other α-spin electrons:

$$V_{\mathrm{ex}}=-e^2\int\int\frac{|\rho_+(r_i,r_j)|^2}{r_{ij}}d\tau_i d\tau_j, \tag{5}$$

where $\rho_+(r_i,r_j)$ is the exchange density between two electrons, one lies in r_i and the another in r_j. In the actual calculation, we also consider their wave function's antisymmetry.

III. CORE SCATTERING AND CLOSED-ORBIT THEORY

The physical picture of the closed-orbit theory can be described as follows: when an atom absorbs a photon, the electron propagates outwards in a near zero-energy Coulomb wave. At sufficiently large distances from the nucleus, the wave propagates semiclassically along classical trajectories with the wave fronts perpendicular to those trajectories. Eventually, the trajectories and their associated waves are turned back by the action of the external fields. Some of the trajectories return to the vicinity of the nucleus and the waves associated with them, which are incoming Coulomb waves, interfere with the outgoing waves, and lead to oscillations in the absorption spectrum. The incoming waves produce Coulomb scattered waves, and for nonhydrogenic atoms, the core-scattered waves. The Coulomb scattered wave is strongly backwardly focused and backtraces the orbit, generating repeated traversals of the trajectory. In this respect, quantum and classical Coulomb scatterings are equivalent. The core-scattered wave redistributes the amplitude of one closed orbit into other closed orbits. Combination orbits are created by scattering of one orbit into another by the core and do not exist in hydrogen. The action of combination orbits is approximately the sum of the consistent hydrogen orbits.

Because the core induces important dynamical effects, it is now apparent that the contribution of the core-scattered waves in any semiclassical approach is necessary to be included. A physical picture of the core-scattering process was first presented by Gao and Delos [5]. We proceed by showing how the core-scattered waves can be dealt with by the closed-orbit theory.

We split the whole space into three characteristic spatial regions: (1) the core region, where the laser field and the core field influences exist, while the external fields can be neglected; (2) the surrounding Coulomb region, where the dynamics of the excited is predominantly determined by the Coulomb force of the ionic core; (3) the outer region, where the influence of the external field is at least as important as the Coulomb force of the ionic core. Our approach is to solve the problem quantum mechanically in the core and Coulomb regions, semiclassically in the Coulomb and outer regions, and then to match these two solutions in the Coulomb region where both are valid.

A. Solution in the core and Coulomb regions

In these regions we can neglect the external field. The core region extends only a few Bohr radii around the atomic nucleus and contains the effect of the laser excitation of the energetically low-lying initial-state wave function. Outside the core region is the surrounding Coulomb region. There we may use quantum-defect theory to obtain an expression for the wave function that is valid throughout the Coulomb region. The general solution at $r=(r,\theta,\varphi)$ can be written as

$$\psi(r)=\phi_0(r)+\sum_j N_j[\psi_j^{(+)}(r)+\psi_j^{(-)}(r)], \tag{6}$$

where $\phi_0(r)$ is the initial outgoing wave, $\psi_j^{(-)}$ is the incoming wave, and $\psi_j^{(+)}$ is the outgoing wave, which arise from the scattering of an electron that approaches the nucleus from a source at infinity.

B. Solution in the Coulomb and outer regions

In the outer region, which typically lies beyond 30 Bohr radii from the nucleus, we can use semiclassical methods to write the wave function as a sum of contributions from classical trajectories, provided we know the wave function on an initial surface. For the system considered here, the Hamiltonian has cylindrical symmetry, so the three-dimensional wave function can be written as

$$\psi_{sc}(r)=\sum_j \psi_0^{(+)}(r_0,\theta_i^j)A_j(r,\theta) \times\exp\left\{i\left[s_j(r,\theta)-\alpha_j\frac{\pi}{2}\right]\right\}e^{im\varphi}, \tag{7}$$

where $\psi_0^{(+)}$ is an outgoing wave function on the initial surface at $r=r_0$. The sum is taken over all trajectories which reach $r=(r,\theta,\varphi)$ having left the surface r_0 at angles θ_i^j to the z axis. The core effects are negligible in this region. The amplitude of the semiclassical wave A_j is given by

$$A_j(r,\theta)=\left|\frac{J_2(0,\theta_i)}{J_2(t,\theta_i)}\right|^{1/2}\left|\frac{r_0^2\sin\theta_i^j}{r^2\sin\theta}\right| \quad (\theta_i^j\neq 0,\pi),$$

where the two-dimensional Jacobian $J_2(t,\theta_i)=\partial(r,\theta)/\partial(t,\theta_i)$ can be calculated from the motion of neighboring trajectories. The phase of the semiclassical wave consists of two terms: the classical action $s_j=\int p_j dq_j$ accumulated along the trajectory j and the Maslov index α_j, which is an integer equal to the number of caustics and foci encountered by the trajectory [1].

C. Matching of solutions

By matching the outgoing components of each of the wave functions in Eqs. (6) and (7) at the starting angles $\theta=\theta_i^j$ of each trajectory which returns to the surface at r_0, we obtain an expression for the outgoing wave function $\psi_0^{(+)}$ on the surface r_0:

$$\psi_0^{(+)}(r_0,\theta_i^j)=\phi_0(r_0,\theta_i^j)+\sum_k N_k\psi_k^{(+)}(r_0,\theta_i^j). \tag{8}$$

Matching the incoming waves at the final angles $\theta=\theta_f^j$ of the returning trajectories gives

$$\psi_{sc}(r_0,\theta_f^j)=N_j\psi_j^{(-)}(r_0,\theta_f^j). \tag{9}$$

On using the expressions for $\psi_0^{(+)}$ and ψ_{sc}, we obtain the following equation for N_j's:

$$\left\{\phi_0(r_0,\theta_i^j)+\sum_k N_k\psi_k^{(+)}(r_0,\theta_i^j)\right\}A_j(r_0,\theta_f^j) \times\exp\left\{i\left[s_j(r,\theta)-\alpha_j\frac{\pi}{2}\right]\right\}=N_j\psi_j^{(-)}(r_0,\theta_f^j). \tag{10}$$

D. Outgoing Coulomb waves

The required asymptotic form for ψ_0 is obtained by considering the action of an outgoing zero-energy Green's function on the dipole operator and initial state [5]:

$$\phi_0(r_0,\theta_i^j)=-i\pi^{1/2}2^{3/4}r_0^{-3/4}e^{i(\sqrt{8r_0}-3\pi/4)}y(\theta_i^j), \tag{11}$$

where the angular functions $y(\theta)=\Sigma_{l=|m|}^{\infty}(-1)^l e^{i\pi\mu_l}B_{lm}Y_{lm}(\theta,0)$ depend on the action of the dipole operator $\hat{D}$, the initial-state wave function ϕ_i, and on the quantum defects μ_l of the ionic core. The coefficients B_{lm} are determined by the photoabsorption process:

$$B_{lm}=\sqrt{8}\int \hat{D}(r')\phi_i(r')R_l^{0,\mathrm{reg}}(r')Y_{lm}^*(\theta',\varphi')dr', \tag{12}$$

where $R_l^{0,\mathrm{reg}}(r)$ is a regular zero-energy radial wave function, outside the ionic core, which can be written as a linear combination of the Bessel functions with prefactors that depend on the quantum defects μ_l:

$$R_l^{0,\mathrm{reg}}(r)=\cos\pi\mu_l\frac{J_{2l+1}(\sqrt{8r})}{(\sqrt{8r})}-\sin\pi\mu_l\frac{H_{2l+1}(\sqrt{8r})}{(\sqrt{8r})}. \tag{13}$$

B_{lm} depends only on the dipole operator and on the initial state. In our calculations, we consider dipole transitions with π-polarized light from an initial s state to final state with magnetic quantum number $m=0$. For this transition, only one B_{lm} coefficient (namely, B_{l0}) is nonzero, leading only to a constant multiplicative factor in the final spectra.

E. Incoming waves

At $r=r_0$, the incoming waves $\psi_j^{(-)}$ are cylindrically modified zero-energy Coulomb waves given by [5]

$$\psi_j^{(-)}(r_0,\theta_f^j)=\begin{cases}(-1)^m\dfrac{\exp\{-i(\sqrt{8r_0}-\pi/2)\}}{\pi\sqrt{8r_0}\sin\theta_f^j} & (\theta_f^j\neq 0,\pi)\\ \dfrac{1}{2}\left(\dfrac{2}{\pi\sqrt{8r_0}}\right)^{1/2}\exp\{-i(\sqrt{8r_0}-\pi/4)\} & (\theta_f^j=0,\pi).\end{cases} \tag{14}$$

F. Outgoing scattered waves

As noted by Gao and Delos, the scattered wave function $\psi_j^{(+)}$ consists of two parts:

$$\psi_j^{(+)} = \psi_{\mathrm{Coul}}^j(r) + \psi_{\mathrm{core}}^j(r). \tag{15}$$

The core-scattered waves $\psi_{\mathrm{core}}^j(r)$ describe the redistribution of amplitude from a trajectory approaching the nucleus along trajectory k into trajectory j, by the compact ionic core and have the partial-wave expansion [5]

$$\psi_{\mathrm{core}}^j(r_0,\theta_i^j) = \left(\frac{2\pi^2}{r_0^3}\right)^{1/4} \sum_{l=|m|}^{\infty} (-1)^{l-m} Y_{lm}^*(\theta_f^k,0) Y_{lm}(\theta_i^j,0) \times e^{i(\sqrt{8r_0}-l\pi-3\pi/4)}(e^{2i\pi\mu_l}-1). \tag{16}$$

The Coulomb scattered wave, $\psi_{\mathrm{Coul}}^j(r)$ is strongly backfocused and on the surface at r_0 is simply related to the incoming wave $\psi_j^{(-)}(r_0,\theta_f^j)$ by

$$\psi_{\mathrm{Coul}}^{(j)}(r_0,\theta_f^j) = \psi_j^{(-)}(r_0,\theta_f^j) e^{i(2\sqrt{8r_0}-\pi)}. \tag{17}$$

Therefore, the Coulomb scattered wave results in the semiclassical wave retracing its path along the closed orbit with a phase change of $(2\sqrt{8r_0}-\pi)$, thus giving rise to repetitions of the orbit. Taking this into account, we see that the dependence of N_j's on $\psi_{\mathrm{Coul}}^j(r)$ can be eliminated simply by including all repetitions of the closed orbits.

G. Oscillator strength

Substituting the above equations into Eq. (5), we arrive at our final iterative equation for N_j's,

$$N_j = \left\{ D_j(\theta_i^j) + \sum_{k,p} N_k B_j^{k,p}(\theta_i^j) \right\} A_j^n \exp\left[i\left(s_j^n - \alpha_j \frac{\pi}{2} - \varphi_j \right) \right], \tag{18}$$

where $\varphi_j = \pi/2$ for $\theta_i^j = 0$ or $\theta_i^j = \pi$ and $\varphi_j = 3\pi/4$ otherwise. For convenience, we have written the core-scattered contributions in the form

$$B_j^{(k,p)}(\theta_i^j) = \begin{cases} i2^{7/4}\pi^{3/2} \sum_{l=|m|}^{\infty} Y_{lm}^*(\theta_f^{k,p},0) Y_{lm}(\theta_i^j,0)(e^{2i\pi\mu_l}-1) & (\theta_f^j \neq 0,\pi), \\ 2^{3/2}\pi \sum_{l}^{\infty} Y_{l0}^*(\theta_f^{k,p},0) Y_{l0}(\theta_i^j,0)(e^{2i\pi\mu_l}-1) & (\theta_f^j = 0,\pi), \end{cases} \tag{19}$$

while the initial outgoing contributions have been expressed as

$$D_j = \begin{cases} 2^{9/4}\pi^{3/2} y(\theta_i^j) & (\theta_i^j \neq 0,\pi), \\ -i4\pi y(\theta_i^j) & (\theta_i^j = 0,\pi). \end{cases}$$

The semiclassical amplitude is now written as

$$A_j^n = \begin{cases} r_0^{1/4} \sin(\theta_f^{j,n}) A_j^n & (\theta_i^j \neq 0,\pi), \\ r_0^{1/2} A_j^n & (\theta_i^j = 0,\pi), \end{cases}$$

where A_j^n, s_j^n, α_j^n, and $\theta_f^{j,n}$ are the amplitude, the action, the Maslov index, and the final return angle, respectively, for the nth return to the nucleus of the jth closed orbit on its return. The contribution from the core-scattered waves also includes a sum over all repetitions [14].

H. Iterative method

We use an iterative procedure to solve Eq. (18) for N_j's, beginning by setting N_k on the right-hand side to be zero and obtain a first approximation to N_j; this is equivalent to the hydrogenic closed-orbit result. In each successive step, extra terms of the form $A_k \ldots A_j e^{i(s_k+\cdots+s_j)}$ are added to the previous result. The resulting recurrence spectrum thus shows two effects not seen in the hydrogenic case. First, the core casts a ''shadow'' in the backward direction changing the recurrence strength of the trajectory that subsequently returns to the core. Second, there are ''combination recurrences'' due to the electron traveling along one closed orbit and then being scattered by the ionic core to another closed orbit. In successive steps of the iterative process combinations of more and more orbits are involved.

Once N_j's have been found, we can obtain the required absorption rate; the oscillatory part of the average oscillator-strength density has the final simple expression [4]

$$f(E) = -\frac{2(E-E_i)}{\pi} \mathrm{lm} \sum_j N_j (-1)^m \sqrt{8}\pi y^*(\theta_f^j), \tag{20}$$

where $y^*(\theta) = \Sigma_{l=|m|}^{\infty} (-1)^l e^{i\pi\mu_l} B_{lm}^* Y_{lm}(\theta,0)$ is the ''uncompleted conjugate'' of $y(\theta)$ [5]. For the photoabsorption from s states using π polarization, only the final states with $m=0$ and odd l are excited and $y^*(\theta)$ takes the form

$$y^*(\theta) = -B_{10} e^{i\pi\mu_l} \sqrt{\frac{3}{4\pi}} \cos\theta. \tag{21}$$

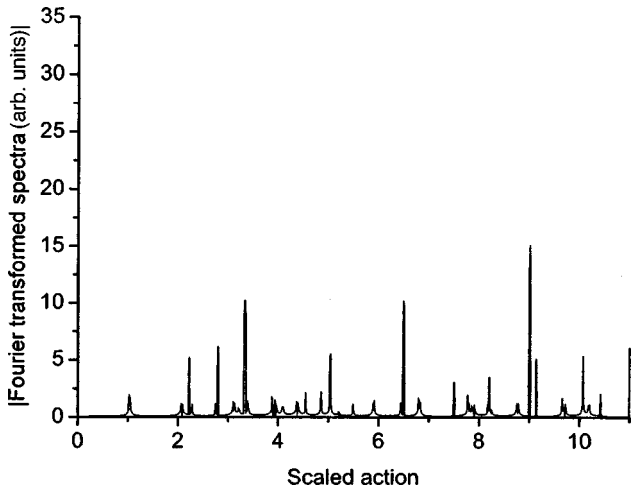

FIG. 1. The Fourier-transformed spectra of the He atom in a magnetic field (without electric field) at scaled energy $\varepsilon=-0.40$. The result is in good agreement with the experimental result [15].

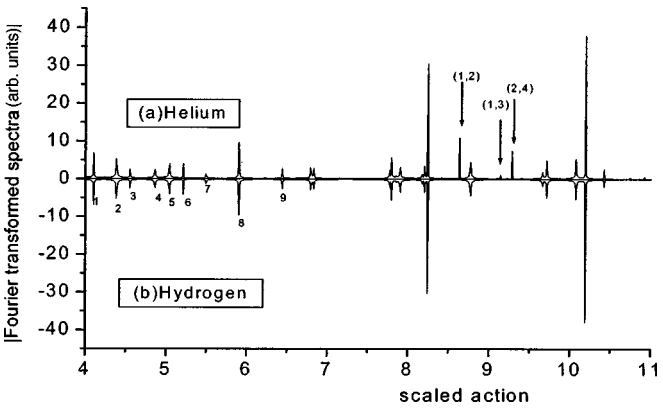

FIG. 2. The Fourier-transformed spectra of the He atom at scaled energy $\varepsilon=-0.586$, the scaled electric field $f=0.068$, $z=\gamma^{-1/3}$ in the range of 34.5–39.9. (a) Calculated recurrence spectra including ionic core-scattered terms (helium); (b) calculated recurrence spectra based on the standard closed-orbit theory (hydrogen).

IV. RECURRENCE SPECTRA AT CONSTANT SCALED ENERGY

A. Hamiltonian and scaled variables

The exact nonrelativistic Hamiltonian for an N-electron atom in parallel electric and magnetic fields, both aligned along the z axis, is described as [6]

$$H_{\text{exact}}=\sum_{i=1}^{N}\frac{p_i^2}{2m}-\sum_{i=1}^{N}\frac{Ze^2}{4\pi\varepsilon_0 r_i}+\sum_{i<j}\frac{e^2}{4\pi\varepsilon_0|\vec{r}_i-\vec{r}_j|}+\sum_{i=1}^{N}\frac{e}{2m}BL_{z,i}+\frac{e^2}{8m}(B^2\rho_i^2+eFz_i). \tag{22}$$

We are dealing with the Rydberg He atom where only one electron is excited to the ionization threshold while the ionic core remains in the ground state. In this situation, the nuclear charge is screened by another electron and the complexity of the exact problem can be simplified to the movement of the highly excited electron in a model potential combined with an external fields. Therefore, the Hamiltonian of the highly excited electron of the He atom in strong parallel electric and magnetic fields (in atomic units) reads

$$H=\frac{1}{2}\left(p_\rho^2+\frac{l_z^2}{\rho^2}\right)+\frac{\gamma}{2}l_z+\frac{1}{8}\gamma^2\rho^2+\frac{1}{2}p_z^2+Fz+V(r), \tag{23}$$

where $\gamma=B/(2.35\times10^5)$ (B is the magnetic-field strength), F is the electric-field strength, for $m=0$ state, $l_z=0$; $V(r)$ is the model potential [Eq. (1)].

The classical motion of Hamiltonian Eq. (23) exhibits an important scaling property. If we transform variables according to $\tilde{r}=r\gamma^{2/3}$, $\tilde{p}=p\gamma^{-1/3}$, $\varepsilon=E\gamma^{-2/3}$, $\tilde{f}=F\gamma^{-4/3}$, $\tilde{t}=t\gamma$, then the classical motion is governed by the scaled Hamiltonian

$$\tilde{H}=\tfrac{1}{2}\tilde{p}_\rho^2+\tfrac{1}{2}\tilde{p}_z^2+\tfrac{1}{8}\tilde{\rho}^2+\tilde{f}\tilde{z}+V(\tilde{r}). \tag{24}$$

If we omit the tilde and rewrite $\tilde{H}$ as ε, we get

$$\varepsilon=\tfrac{1}{2}p_\rho^2+\tfrac{1}{2}p_z^2+\tfrac{1}{8}\rho^2+fz+V(r). \tag{25}$$

From Eq. (25), we find that the scaled Hamiltonian does not depend on the energy E and field strength separately but only on the scaled energy ε and the scaled electric field f, thus reducing parameter B.

B. Closed-orbit search

In order to solve numerically the motion equations and remove the Coulomb singularity generated by Hamiltonian (25) it is convenient to make a regularizing transformation. For the case considered here, where $m=0$, we implement the Kustaanheimo-Stiefel transformation [7], which transforms the system from a three-dimensional to a four-dimensional one. Introducing a time-dilation variable in this higher-dimensionality representation removes the Coulomb singularity at the origin. Removal of the Coulomb singularity makes the numerical calculation very stable and an orbit launched from the origin can evolve quite a long time without loss of numerical accuracy.

Due to the increased dimensionality of the phase space involved, the number of the closed orbits will be large. In our calculation, we take $\varepsilon=-0.586$, $f=0.068$ and constrain ourselves to those closed orbits with scaled actions smaller than 20. For each orbit, we evaluated the classical action, the classical amplitude A, as well as the Maslov index α. Some of the orbits are given in Fig. 3.

C. Recurrence spectra at constant scaled energy

The oscillatory part of the density of oscillator strength has been given in Eq. (20), after an iterative process for N_j's is carried out and the scaling is used, it can be written as

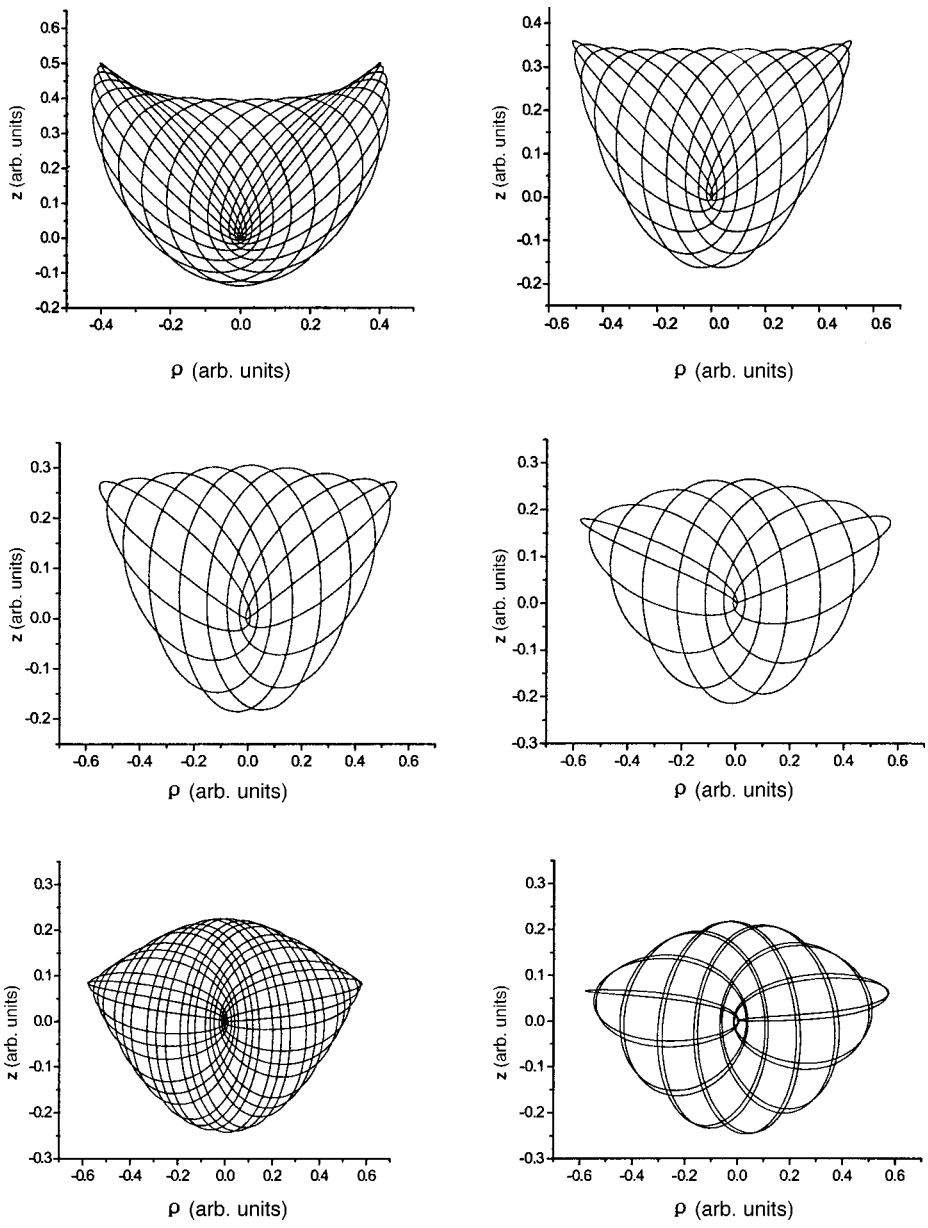

FIG. 3. Some closed orbits of helium in parallel electric and magnetic fields at scaled energy $\varepsilon=-0.586$. The orbits are plotted in the ρ-z plane.

$$f(z)=\sum_j C_j \sin\left(2\pi\tilde{s}_j z-\frac{\alpha_j\pi}{2}-\varphi_j+2\pi\mu_l\right), \quad (26)$$

where $z=\gamma^{-1/3}$, $\tilde{S}_j$ is the scaled action. The quantum defects μ_l can be calculated by the following equation [6]:

$$\mu_l=\frac{\sqrt{2}}{\pi}\lim_{R\to\infty}\left[\int_{r_0}^{R}\sqrt{-V(r)-\frac{(l+1/2)^2}{2r^2}}\,dr-\int_{r_0}^{R}\sqrt{-\frac{1}{r}-\frac{(l+1/2)^2}{2r^2}}\,dr\right], \quad (27)$$

where $r_0=1/2(l+1/2)^2$ is the classical turning points depending on l.

The Fourier transform recurrence spectra can be calculated in the interval $[z_1, z_2]$. With $\tilde{z}=1/2(z_1+z_2)$ and $\Delta z=z_2-z_1$, we obtain

$$\begin{aligned}F(\tilde{s})&=\frac{1}{\Delta z}\int_{z_1}^{z_2}f(z)e^{2\pi i\tilde{s}(z-\tilde{z})}dz=\frac{1}{\Delta z}\int_{z_1}^{z_2}e^{2\pi i\tilde{s}(z-\tilde{z})}\sum_j C_j\\&\quad\times\sin\left(2\pi\tilde{s}_j z-\frac{\alpha_j\pi}{2}-\varphi_j+2\pi\mu_l\right)dz\\&=\sum_j C_j\frac{\sin[\pi(\tilde{s}-\tilde{s}_j)\Delta z]}{2\pi(\tilde{s}-\tilde{s}_j)\Delta z}\\&\quad\times\exp\left[-i\left(2\pi\tilde{s}_j z-\frac{\alpha_j\pi}{2}-\varphi_j+2\pi\mu_l\right)\right]. \quad (28)\end{aligned}$$

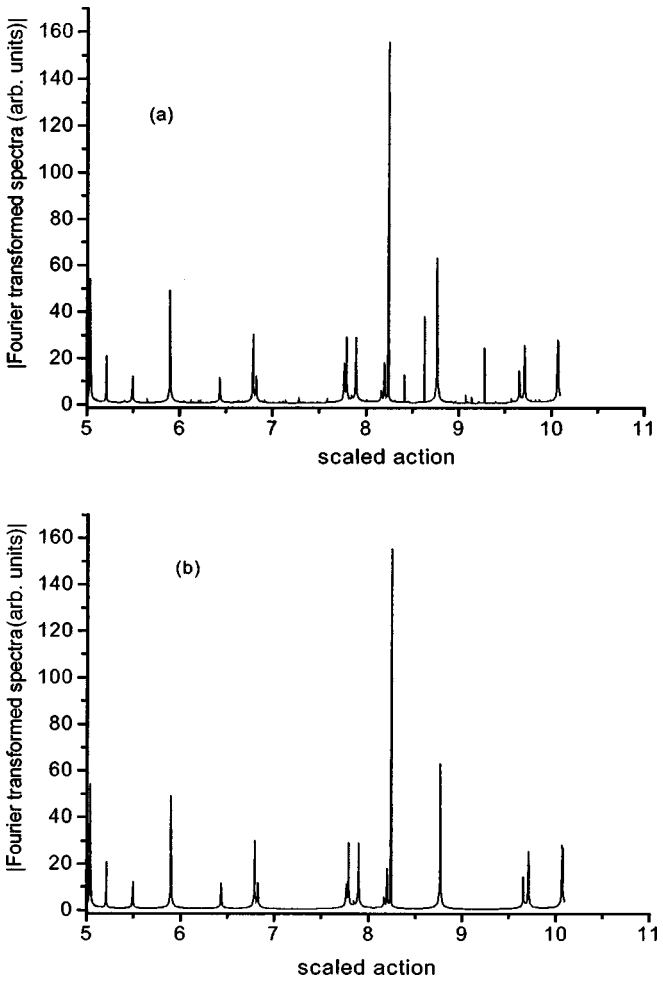

FIG. 4. The Fourier-transformed spectra of the He atom at scaled energy $\varepsilon=-3.0$, the scaled electric field $f=0.068$, $z=\gamma^{-1/3}$ in the range of 34.5–39.9. (a) Calculated recurrence spectra considering the influence of the electron exchange; (b) calculated recurrence spectra without the influence of the electron exchange.

For finite length Δz, $F(\tilde{s})$ are complex numbers. In our calculation, we take the absolute value of $F(\tilde{s})$.

D. The influence of the exchange potential on the spectra

Considering the electron exchange potential, the quantum defect for helium separates into two parts $\mu_l=\mu_C+\mu_{\rm ex}$: one from electron exchange $\mu_{\rm ex}$ and a direct Coulomb part μ_C. The electron exchange $\mu_{\rm ex}$ term, due to the requirement of antisymmetrization of the total wave function imposed by the Pauli exclusion principle, is responsible for the spin-dependent effects in our recurrence spectra. For example, for the $l=1$ state, $\mu_C=0.024$, while $\mu_{\rm ex}=0.04$, thus, the main contribution to the quantum defect comes from the $\mu_{\rm ex}$ term. In addition, after including the exchange potential, the number of the closed orbits increases, which results in more peaks in the recurrence spectra.

V. RESULTS AND DISCUSSION

In Fig. 1, we calculate the scaled recurrence spectra of the He atom in the magnetic field (without electric field) at scaled energy $\varepsilon=-0.40$. The result is in good agreement with the experimental Fourier-transformed spectra given by Karremans *et al.* [15]; for example, the peaks in the recurrence spectra of our result and the experimental one occur nearly at the same position, which suggests that our method is correct. Figure 2 gives the Fourier-transformed spectra of the He atom in parallel electric and magnetic fields at scaled energy $\varepsilon=-0.586$, the scaled electric field $f=0.068$, $z=\gamma^{-1/3}$ in the range of 34.5–39.9 and the spectra are compared with the hydrogen case. Figure 2(a) is the recurrence spectra of the He atom and (b) is the recurrence of the H atom using the standard closed-orbit theory. One can see that for smaller $\tilde{s}$, the spectra structures of He and H atoms are analogous. As $\tilde{s}$ is increased, there are substantial discrepancies between them, which shows that the dynamics of the He atom in strong external fields is inherently chaotic. Each resonance peak in the Fourier-transformed spectra is associated with classical closed orbit. Some of the orbits are drawn in Fig. 3. The integers in the Fig. 2 indicate primary orbits. Each pair of integers in the figures indicates the combination of two orbits, corresponding to a core-scattered peak. In fact this phenomenon could be attributed to the combination recurrence. For example, the peak marked by the arrow at (1, 2) is located at $\tilde{s}_1+\tilde{s}_2\approx 8.6$, while the peak (2, 4) is located at $\tilde{s}_2+\tilde{s}_4\approx 9.2$. Figure 4 gives the different recurrence spectra of the He atom with or without the influence of the electron exchange. Figure 4(a) is the recurrence spectra considering the influence of the electron exchange; Fig. 4(b) is the recurrence spectra without the influence of the electron exchange. From the figures we can see, once considering the electron exchange effect, that more pronounced peaks appear in the recurrence spectra. This effect results from the interference between hydrogenic orbits and core-scattered combination orbits, and demonstrate the sensitivity of recurrence strength to the spatial symmetry of the wave function imposed by the Pauli exclusion principle.

VI. CONCLUSION

A model potential for the general Rydberg atom is put forward. By using this potential and a different scaled transformation, we calculated the recurrence spectra of the He atom in parallel electric and magnetic fields. The non-Columbic nature of the ionic core has been considered in classical trajectory calculations and families of core-scattered nonhydrogenic closed orbits have been discovered. The resonance structures in the Fourier-transformed spectra of the He atom have been recently denoted as effects resulting from the core scattering of returning waves at the ionic core [3], from which we gain a deeper understanding of the behavior of multielectron Rydberg atoms in strong external fields. The good agreement between the experimental recurrence spectra and the spectra in our paper for the He atom in a magnetic field without an electric field demonstrates the correctness of our method. Presently, no experiments on the recurrence spectra of He atom in parallel electric and magnetic fields have been carried out. Our predication shows that there are interesting phenomena here, and we hope that our calculations may guide future measurements.

ACKNOWLEDGMENTS

This work was supported by the National Science Foundation of China (Grant No. 20173031), the Science Foundation of Shandong Province of China and the Doctoral Foundation of the Ministry of Education of People's Republic of China. We are grateful to S. L. Lin and M. L. Du for valuable discussions.

[1] M. L. Du and J. B. Delos, Phys. Rev. A **38**, 1896 (1988); **38**, 1913 (1988).
[2] Z. Y. Liu *et al.*, Phys. Rev. A **54**, 4078 (1996); **55**, 4605 (1997); **56**, 2670 (1997).
[3] Lin Sheng-Lu *et al.*, Chin. Phys. Lett. **19**, 29 (2002).
[4] P. A. Dando *et al.*, Phys. Rev. A **54**, 127 (1996).
[5] J. Gao and J. B. Delos, Phys. Rev. A **46**, 1449 (1992); **46**, 1455 (1992).
[6] Bruno Hupper, Jong Main, and Gunter Wumner, Phys. Rev. A **53**, 744 (1996).
[7] Jianguo Rao and K. T. Taylor, J. Phys. B **35**, 2627 (2002).
[8] A. Kips, W. Vassen, and W. Hogervorst, Phys. Rev. A **58**, 3043 (1998).
[9] K. Karremans *et al.*, Phys. Rev. A **60**, R2649 (1999).
[10] A. Kips, W. Vassen, and W. Hogervorst, Phys. Rev. A **59**, 2948 (1999).
[11] A. Kips, W. Vassen, and W. Hogervorst, Phys. Rev. A **60**, 4764 (1999).
[12] M. Keeler and T. J. Morgan, Phys. Rev. Lett. **80**, 5726 (1998).
[13] P. Gombas, The Questions of Multi-Particle Systems in Quantum-Mechanics (unpublished).
[14] J. M. Mao, J. Shaw, and J. B. Delos, J. Stat. Phys. **68**, 51 (1992).
[15] K. Karremans, A. Kips, W. Vassen, and W. Hogervorst, Phys. Rev. A **60**, 4764 (1999).